ARTICLE
Journal of Cellular Biochemistry 113:1377–1385 (2012)

Journal of Cellular Biochemistry

Ca^{2+} Store Depletion and Endoplasmic Reticulum Stress are Involved in P2X7 Receptor-Mediated Neurotoxicity in Differentiated NG108-15 Cells

Chia-Chia Chao,[1] Chieh-Chen Huang,[1] Dah-Yuu Lu,[2] Kar-Lok Wong,[3] Yun-Ru Chen,[3] Tzu-Hurng Cheng,[4] and Yuk-Man Leung[1*]

[1]*Department of Life Sciences, National Chung Hsing University, Taichung, 402, Taiwan*
[2]*Graduate Institute of Neural and Cognitive Sciences, China Medical University, Taichung 40402, Taiwan*
[3]*Department of Anesthesiology, China Medical University, Taichung 40402, Taiwan*
[4]*Department of Biological Sciences and Technology, China Medical University, Taichung 40402, Taiwan*

ABSTRACT

P2X7 receptor (P2X7R) activation by extracellular ATP triggers influx of Na^+ and Ca^{2+}, cytosolic Ca^{2+} overload and consequently cytotoxicity. Whether disturbances in endoplasmic reticulum (ER) Ca^{2+} homeostasis and ER stress are involved in P2X7R-mediated cell death is unknown. In this study, a P2X7R agonist (BzATP) was used to activate P2X7R in differentiated NG108-15 neuronal cells. In a concentration-dependent manner, application of BzATP (10–100 μM) immediately raised cytosolic Ca^{2+} concentration ($[Ca^{2+}]_i$) and caused cell death after a 24-h incubation. P2X7R activation for 2 h did not cause cell death but resulted in a sustained reduction in ER Ca^{2+} pool size, as evidenced by a diminished cyclopiazonic acid-induced Ca^{2+} discharge (fura 2 assay) and a lower fluorescent signal in cells loaded with Mag-fura 2 (ER-specific Ca^{2+}-fluorescent dye). Furthermore, P2X7R activation (2 h) led to the appearance of markers of ER stress [phosphorylated α subunit of eukaryotic initiation factor 2 (p-eIF2α) and C/EBP homologous protein (CHOP)] and apoptosis (cleaved caspase 3). Xestospongin C (XeC), an antagonist of inositol-1,4,5-trisphosphate (IP_3) receptor (IP3R), strongly inhibited BzATP-triggered $[Ca^{2+}]_i$ elevation, suggesting that the latter involved Ca^{2+} release via IP3R. XeC pretreatment not only attenuated the reduction in Ca^{2+} pool size in BzATP-treated cells, but also rescued cell death and prevented BzATP-induced appearance of ER stress and apoptotic markers. These novel observations suggest that P2X7R activation caused not only Ca^{2+} overload, but also Ca^{2+} release via IP3R, sustained Ca^{2+} store depletion, ER stress and eventually apoptotic cell death. J. Cell. Biochem. 113: 1377–1385, 2012.

KEY WORDS: P2X7 RECEPTOR; Ca^{2+} STORE; ENDOPLASMIC RETICULUM STRESS

In brain ischemia or in stroke, excitotoxicity occurs when hyperactivation of glutamate receptors leads to cytosolic Ca^{2+} overload and neuronal cell death. What aggravates the pathology is that during brain ischemia/hypoxia, extracellular ATP level also increases [Skaper et al., 2010]. Pathologically high levels of ATP could lead to or worsen excitotoxicity [Matute et al., 2007; Skaper et al., 2010]. One subtype of ATP receptors, namely, the P2X7 receptor (P2X7R), has millimolar affinity to ATP and has been implicated in neurotoxicity. For instance, P2X7R stimulation in vivo is lethal to rat retinal ganglion neurons [Hu et al., 2010] and there is evidence that this P2X7R lethal action to rat retinal neurons is relevant in hypoxic conditions [Sugiyama et al., 2010]. Activation of the P2X7R, together with nerve growth factor, aggravates hypoglycemia-induced cell death in cerebellar granule neurons [Cavaliere et al., 2002]. What worsens the situation is that during cerebral ischemia, P2X7R have been shown to be up-regulated [Franke et al., 2004]. Furthermore, in vitro ischemia has also been shown to even enhance the sensitivity of P2X7R to ATP [Wirkner et al., 2005].

P2X7R is a non-selective cation channel pore that allows the influx of Na^+ and Ca^{2+}; it is a homotrimer that becomes activated upon the binding of three ATP molecules [Browne et al., 2010]. Although cytosolic Ca^{2+} overload is a likely contributing factor in P2X7R toxicity, whether perturbations in organelle Ca^{2+} are also

Conflict of interest: None.
Grant sponsor: National Science Council of Taiwan; Grant number: NSC 100-2320-B-039-006-.
*Correspondence to: Prof. Yuk-Man Leung, Graduate Institute of Neural and Cognitive Sciences, China Medical University, Taichung 40402, Taiwan. E-mail: ymleung@mail.cmu.edu.tw
Received 20 November 2011; Accepted 22 November 2011 • DOI 10.1002/jcb.24010 • © 2011 Wiley Periodicals, Inc.
Published online 1 December 2011 in Wiley Online Library (wileyonlinelibrary.com).

involved is unknown. Part of the endoplasmic reticulum (ER) performs the function of intracellular Ca^{2+} storage and is responsive to certain hormones or neurotransmitters. The latter, by activating G-protein-coupled receptors that are associated with phospholipase C, generates inositol-1,4,5-trisphosphate (IP_3) from phosphatidyl-4,5-bisphosphate (PIP_2) cleavage. IP_3 binds to its receptor (IP3R, itself a Ca^{2+} release channel) in the ER and mobilizes Ca^{2+} from intracellular Ca^{2+} stores [Berridge, 2009]. After Ca^{2+} mobilization from the store by IP_3, the emptiness of the Ca^{2+} store triggers the opening of a store-operated Ca^{2+} channel (SOC) at the plasma membrane to refill the Ca^{2+} store [Berridge, 2009; Varnai et al., 2009].

Stress to the ER could occur when there is an overload of protein synthesis, protein malfolding, or chronic depletion of Ca^{2+} storage [Harding and Ron, 2002]. Whether, or to what extent, ER stress contributes to excitotoxicity in neurons is not fully understood. For instance, whether glutamate-mediated neuronal excitotoxicity involves ER stress still remains controversial. Kainic acid, a glutamate receptor sub-type agonist, causes hippocampal neuronal cell death, disintegration of the ER membrane, and appearance of ER stress proteins such as Bip, CHOP, and caspase-12 [Sokka et al., 2007]. On the contrary, N-methyl-D-aspartate (NMDA) receptor-mediated excitotoxic apoptosis in vitro and in vivo occurs without any indication of ER stress [Concannon et al., 2008]. Hitherto no information is available on whether P2X7R-mediated neurotoxicity involves chronic Ca^{2+} store depletion and ER stress. In the present work we investigated this issue using differentiated NG108-15 cells. NG108-15 is a neuroblastoma-glia hybrid, which when differentiated, develops neuronal characteristics (substantial and long neurite generation). NG108-15 cells have been shown to possess P2X7R [Watano et al., 2002]. We observed that stimulation of the P2X7R by 2′,3′-O-(4-benzoylbenzoyl)-ATP (BzATP, a selective P2X7R agonist) could cause Ca^{2+} influx and substantial cytotoxicity in differentiated NG108-15 cells. BzATP challenge also resulted in sustained Ca^{2+} store depletion and ER stress. Remarkably, pharmacological blockade of Ca^{2+} release via IP3R prevented BzATP-induced Ca^{2+} store depletion, ER stress, and apoptotic cell death. The mechanisms by which BzATP-induced cell death may involve sustained Ca^{2+} store depletion and ER stress will be discussed.

MATERIALS AND METHODS

CELL CULTURE

NG108-15 cells were grown at 37°C in 5% CO_2 in Dulbecco's modified Eagle's medium (DMEM) supplemented with 10% fetal bovine serum (Invitrogen, Carlsbad, CA) and penicillin-streptomycin (100 units/ml, 100 μg/ml) (Invitrogen). These cells were induced to differentiate into more mature neurons by being incubated in the above-mentioned medium with 0.1% fetal bovine serum, 10 μM retinoic acid, and 30 μM forskolin for 3 days; then the neuron morphology could be observed with the extensive generation of neurites.

ASSAY OF CELL VIABILITY

Cell viability was examined by the 3-(4,5-dimethylthiazol-2-yl)-2,5-diphenltetrazolium bromide (MTT) method or trypan blue exclusion method. In the MTT assay, cells were cultured in a 96-well plate at a density of 1.5×10^4/well, and were then treated with or without BzATP for 24 h. MTT (final concentration at 0.5 mg/ml) was subsequently added to each well and then further incubated for 4 h. The culture medium was then removed and 100 μl of DMSO was added to each well for 15 min (with shaking) to dissolve the cells. The absorbance at 595 nm was measured using an ELISA reader and was used as an indicator of cell viability.

MICROFLUORIMETRIC MEASUREMENT OF CYTOSOLIC Ca^{2+}

Microfluorimetric measurement of cytosolic Ca^{2+} concentration ($[Ca^{2+}]_i$) was performed using fura-2 as the Ca^{2+}-sensitive fluorescent dye as described previously [Leung et al., 2002; Leung et al., 2011]. Briefly, cells were incubated with 5 μM fura-2 AM (Invitrogen, Carlsbad, CA) for 1 h at 37°C and then washed and bathed in extracellular bath solution which contained (mM): 140 NaCl, 4 KCl, 1 $MgCl_2$, 2 $CaCl_2$, 10 HEPES (pH 7.4 adjusted with NaOH). When intracellular Ca^{2+} release was assayed, a Ca^{2+}-free solution, which was the same as the extracellular bath solution mentioned above except that Ca^{2+} was omitted and 20 μM EGTA was supplemented, was used. Cells were alternately excited with 340 and 380 nm using an optical filter changer (Lambda 10-2, Sutter Instruments). Emission was collected at 500 nm and images were captured using a CCD camera (CoolSnap HQ2, Photometrics, Tucson, AZ) linked to an inverted Nikon TE 2000-U microscope. Images were analyzed with an MAG Biosystems Software (Sante Fe, MN). All imaging experiments were performed at room temperature (~25°C).

MICROFLUORIMETRIC MEASUREMENT OF ER Ca^{2+}

Microfluorimetric measurement of ER Ca^{2+} concentration was performed using Mag-fura-2 as the Ca^{2+}-sensitive fluorescent dye using protocols suggested previously [Gerasimenko and Tepikin, 2005]. Briefly, cells were incubated with 5 μM Mag-fura-2 AM (Invitrogen) for 1 h at 37°C and then washed. Cells were treated with or without drugs for 2 h and before measurements the cells were permeabilized and washed with a digitonin (10 μM)-containing intracellular solution which contained (mM): 140 KCl, 8 NaCl, 1 $MgCl_2$, 1.85 EGTA, 1 $CaCl_2$, 10 HEPES, and 8 MgATP (pH 7.25 adjusted with KOH). The free Ca^{2+} concentration in this intracellular solution was calculated to be 114 nM. Mag-fura-2 preferentially accumulates in the ER yet a very small percentage of the dye might stay in the cytosol. To remove any Mag-fura-2 acid in the cytosol, cells were carefully and thoroughly washed a few times in the above-mentioned intracellular solution to allow cytosolic Mag-fura-2 to diffuse out across the digitonin-permeabilized plasma membrane. Imaging experiments were performed with the same procedures as described above for microfluorimetric measurement of cytosolic Ca^{2+}.

WESTERN BLOT

Western blot was performed as described previously [Lu et al., 2009]. Briefly, cells were washed in cold phosphate-buffered saline (PBS) solution, lysed for 30 min on ice with radioimmunoprecipitation assay (RIPA) buffer. Samples containing 30 μg protein were separated on 10% sodium dodecyl sulfate-polyacrylamide gels (SDS–PAGE) and transferred to polyvinylidene difluoride (PVDF)

membranes (Millipore, Bedford, MA). The membranes were incubated for 1 h with 5% nonfat milk in PBS buffer to block nonspecific binding. The membranes were incubated with primary antibodies: Anti-β-actin (1:5000; Santa Cruz Biotechnology), anti-eIF-2α (1:1000; Cell Signaling Technology), anti-phosphorylated eIF-2α (1:1000; Cell Signaling Technology), anti-CHOP (1:1000; Santa Cruz Biotechnology), anti-caspase-3 and anti-cleaved caspase-3 (1:1000; Santa Cruz Biotechnology) for 2 h. Subsequently, the membranes were incubated with goat anti-rabbit or goat anti-mouse peroxidase-conjugated secondary antibodies (1:10000; Santa Cruz Biotechnology) for 1 h. The blots were visualized by enhanced chemiluminescence (ECL; Millipore) using Kodak X-OMAT LS film (Eastman Kodak, Rochester).

STATISTICAL ANALYSIS

Data are presented as mean ± SEM. The unpaired or paired Student's *t*-test was used where appropriate to compare two groups. ANOVA was used to compare multiple groups, followed by the Tukey's HSD post-hoc test. A value of $P < 0.05$ was considered to represent a significant difference.

RESULTS

BzATP, a selective P2X7R agonist, concentration-dependently caused cell death in differentiated NG108-15 cells after 24 h (Fig. 1A). Of the P2X receptors, only the P2X7R has millimolar affinity for ATP [Jarvis and Khakh, 2009]. We observed that significant cell death in differentiated NG108-15 cells required millimolar levels of extracellular ATP (cell death = 27 ± 3.1 and 62 ± 1% at 0.3 and 1 mM ATP, respectively; three independent experiments), therefore confirming that cytotoxicity was due to P2X7R activation. When differentiated NG108-15 cells were treated with 100 μM BzATP for only 2 h, there was no cell death (Fig. 1B). However, when the cells, having been exposed to 100 μM BzATP for 2 h, were washed out of the agonist and further incubated for 22 h, there was substantial cell death (Fig. 1C). This suggests that cytotoxic signals or certain forms of damage had already been generated after a 2-h exposure to BzATP.

Since P2X7R is a cation channel which is permeable to Ca^{2+}, we next examined the effects of BzATP on $[Ca^{2+}]_i$. Figure 2A–C shows that BzATP treatment caused a slow elevation in $[Ca^{2+}]_i$ in a concentration-dependent manner. The gradual dilation of the P2X7R pore may account for the slow elevation in $[Ca^{2+}]_i$. The elevation in $[Ca^{2+}]_i$ appeared to be due to Ca^{2+} influx since at 100 μM, BzATP did not cause $[Ca^{2+}]_i$ elevation in Ca^{2+}-free bath solution (data not shown). Cytotoxicity (Fig. 1A) correlated well with the ability of BzATP to cause $[Ca^{2+}]_i$ elevation (Fig. 2A–D). The BzATP-triggered Ca^{2+} signal was sustained even after 2 h of agonist exposure (Fig. 2E; note that in the BzATP-treated group, the cells were still exposed to 100 μM BzATP when imaged for $[Ca^{2+}]_i$).

As the cells remained viable after a 2-h BzATP challenge (Fig. 1B) but had apparently received cytotoxic signals (Fig. 1C), experiments were conducted to examine if there was a perturbation in $[Ca^{2+}]_i$ homeostasis in BzATP-treated cells for 2 h. Fura-2-loaded cells were treated with or without 100 μM BzATP for 2 h, then washed in and

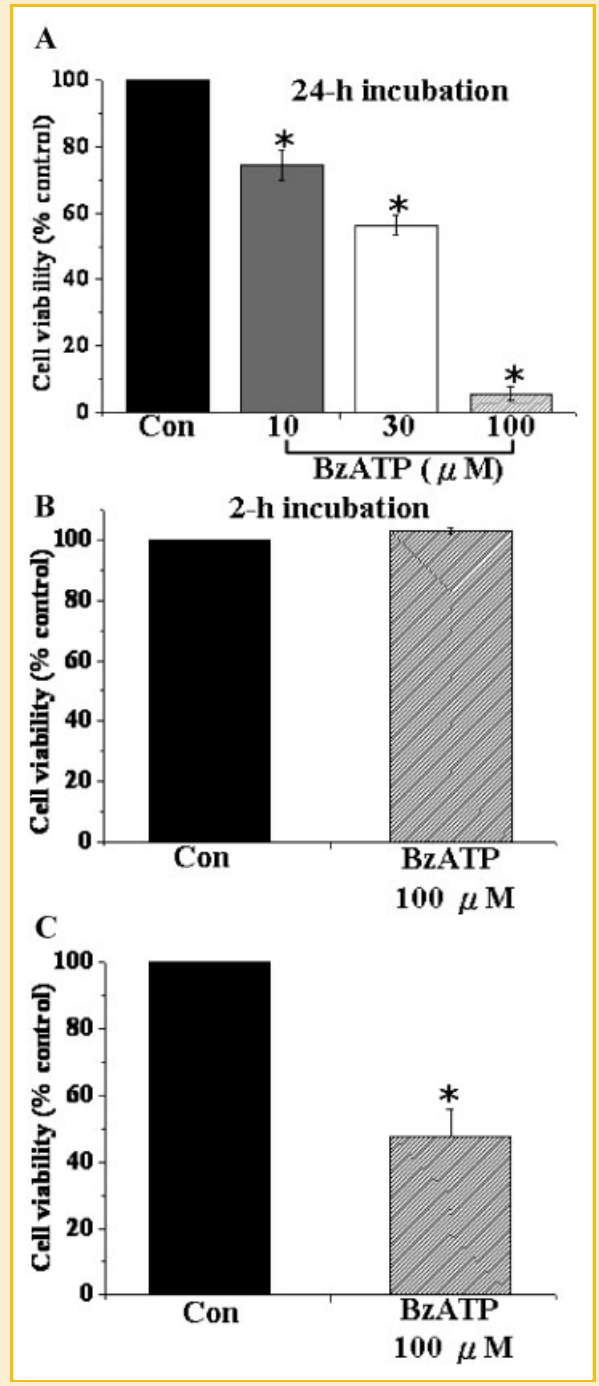

Fig. 1. BzATP caused cytotoxicity in differentiated NG108-15 cells. A: Cells were incubated with 0, 10, 30, or 100 μM BzATP for 24 h and cell viability was determined by the MTT assay. B: Cells were treated with or without 100 μM BzATP for 2 h and cell viability was determined by trypan blue exclusion test. C: Cells were treated with or without 100 μM BzATP for 2 h, BzATP was then washed out and the cells were further incubated in control medium for 22 h before trypan blue exclusion test. Results are mean ± SEM from four to five separate experiments. Asterisks indicate statistical significance ($P < 0.05$) in comparison to the control.

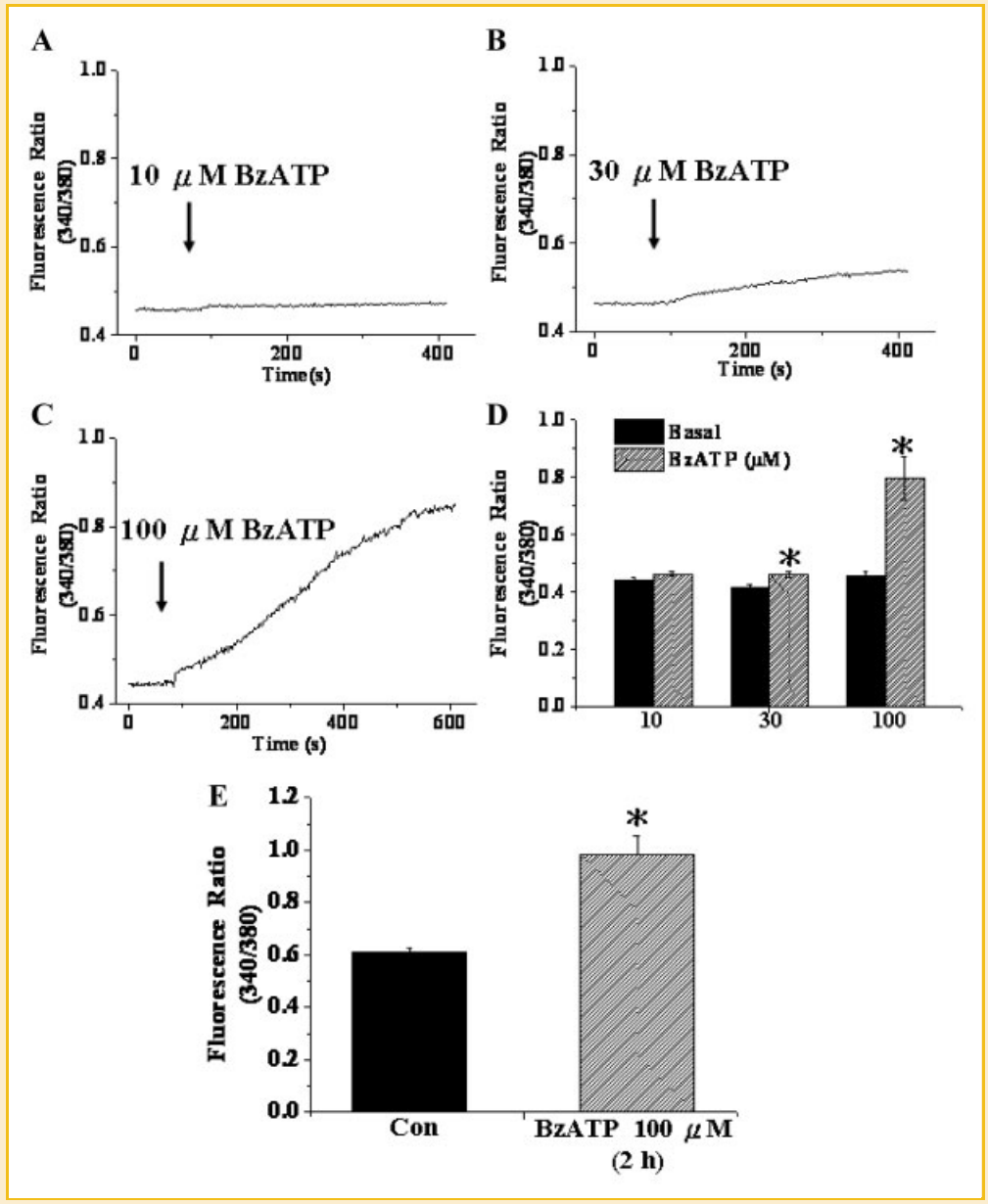

Fig. 2. $[Ca^{2+}]_i$ was increased concentration-dependently by BzATP in differentiated NG108-15 cells. A–C: Cells were assayed for $[Ca^{2+}]_i$ microfluorimetrically using fura 2 in Ca^{2+}-containing bath solution and were challenged with 10, 30 or 100 μM BzATP. D: Results from A–C were quantified. E: Cells were treated with or without 100 μM BzATP for 2 h and then assayed for $[Ca^{2+}]_i$. In the BzATP-treated group, the cells were still exposed to 100 μM BzATP when imaged for $[Ca^{2+}]_i$. In each group, results are mean ± SEM of 20–36 cells from five separate experiments. Asterisks indicate statistical significance ($P < 0.05$) in comparison to the basal level or control.

finally bathed in Ca^{2+}-containing bath solution. As shown in Figure 3, basal $[Ca^{2+}]_i$ in both control and BzATP groups were comparable, suggesting that: (1) The effect of BzATP was reversible upon washing even after 2 h of incubation, (2) the plasma membrane of the BzATP-treated cells appeared to be functionally intact (dysfunctional plasma membrane should have lost its ability to maintain a steep Ca^{2+} gradient across the plasmalemma). The data implicate that Ca^{2+} extrusion (via plasmalemmal Ca^{2+} pump and/or Na^{+}-Ca^{2+} exchanger) was probably fully operative. KCl-induced (iso-osmotic substitution) depolarization triggered comparable Ca^{2+} signals (Ca^{2+} influx via voltage-gated Ca^{2+} channels) in both control and BzATP-treated cells (2 h). The above findings suggest that the plasma membrane of BzATP-treated cells (2 h) was still likely to possess functional integrity.

We then examined whether intracellular Ca^{2+} stores were perturbed in BzATP-treated cells (Fig. 4A–C). Fura-2-loaded cells were treated with or without 100 μM BzATP for 2 h, then washed in Ca^{2+}-containing bath solution and finally bathed in Ca^{2+}-free bath solution. The cells were challenged with a maximal concentration of cyclopiazonic acid (CPA, 50 μM), which discharged the Ca^{2+} stores by inhibiting the sarcoplasmic/ER Ca^{2+}-ATPases (SERCA). Whilst the basal Ca^{2+} levels in both groups of cells were

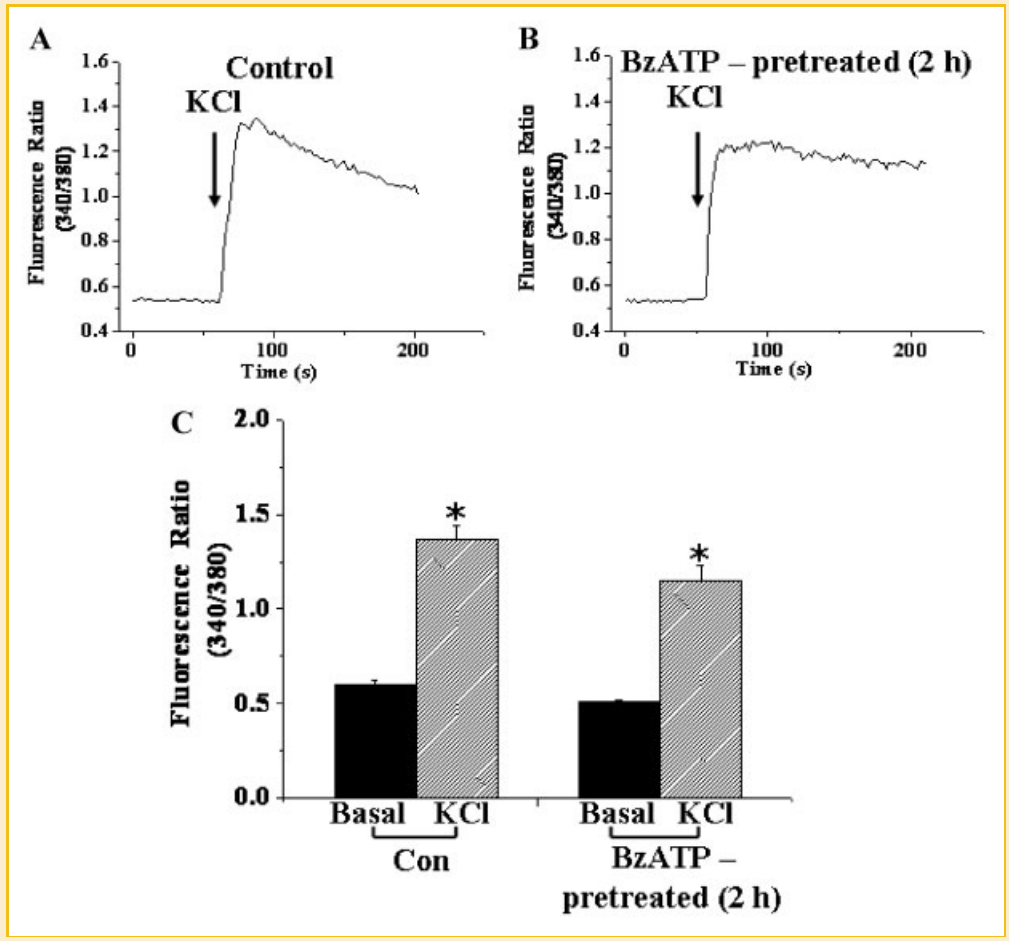

Fig. 3. KCl-triggered $[Ca^{2+}]_i$ responses in differentiated NG108-15 cells pretreated with or without BzATP for 2 h. Control cells (A) or cells pretreated with 100 μM BzATP for 2 h (B) were assayed for $[Ca^{2+}]_i$ in Ca^{2+}-containing bath solution and stimulated with 70 mM KCl (iso-osmotic substitution). C: Results from (A) and (B) are quantified. In each group, results are mean ± SEM of 33–48 cells from four separate experiments. Asterisks indicate statistical significance ($P < 0.05$) in comparison to the basal level.

not significantly different, CPA-induced Ca^{2+} release was much reduced in the BzATP-treated cells ($P < 0.05$), suggesting that for the latter group, the Ca^{2+} stores had been markedly reduced in functional size (despite that the Ca^{2+} stores had been allowed to refill during the washing in Ca^{2+}-containing solution). Subsequent to Ca^{2+} store discharge, Ca^{2+} was replenished to the bath solution to observe store-operated Ca^{2+} entry. Interestingly, the latter was much attenuated in the BzATP-treated cells ($P < 0.05$).

To confirm that the Ca^{2+} store was depleted in BzATP-treated cells (2 h), the Ca^{2+} level in the ER Ca^{2+} pool was examined using the Mag-fura-2 technique. As explained in the Methods section, this Ca^{2+}-sensitive dye preferentially accumulates in the ER; the minute amount of cytosolic Mag-fura-2 could be washed away through very small leak openings in the digitonin-permeabilized membranes when the cells were washed in intracellular solution containing 10 μM digitonin. Thus, Mag-fura-2-loaded cells were treated with or without 100 μM BzATP for 2 h, then permeabilized and washed with a digitonin-containing intracellular solution. ER Ca^{2+} concentration was found to be significantly lower in BzATP-treated cells (Fig. 4D).

The mechanism by which BzATP caused Ca^{2+} store depletion was next investigated. There are at least three types of channels to permit Ca^{2+} to flow out of the store: Unknown leak channels, ryanodine receptor-channels (RYR) and IP3R. No pharmacological tools are known to inhibit the unknown leak channels. There appeared to be no functional RYR in differentiated NG cells, since the agonist caffeine (at 20 mM) failed to elicit any Ca^{2+} signal (data not shown). We then proceeded to use an antagonist of IP3R, xestospongin (XeC), to examine if IP3R was involved. It was observed that XeC substantially reduced the $[Ca^{2+}]_i$ elevation elicited by BzATP (Fig. 5A–C; $P < 0.05$). Therefore, BzATP-triggered $[Ca^{2+}]_i$ elevation involved in part Ca^{2+} release via IP3R. Together with the observation that BzATP did not trigger $[Ca^{2+}]_i$ elevation in Ca^{2+}-free solution, our data suggest that BzATP might initially cause an influx of Ca^{2+} from the extracellular milieu, and such Ca^{2+} influx subsequently triggered Ca^{2+} release via IP3R (see Discussion section). Of note, we also found that XeC substantially reduced the CPA-induced Ca^{2+} signal in Ca^{2+}-free solution (Fig. 5D–F; $P < 0.05$), suggesting that Ca^{2+} release via IP3R was also involved in CPA-induced Ca^{2+} discharge.

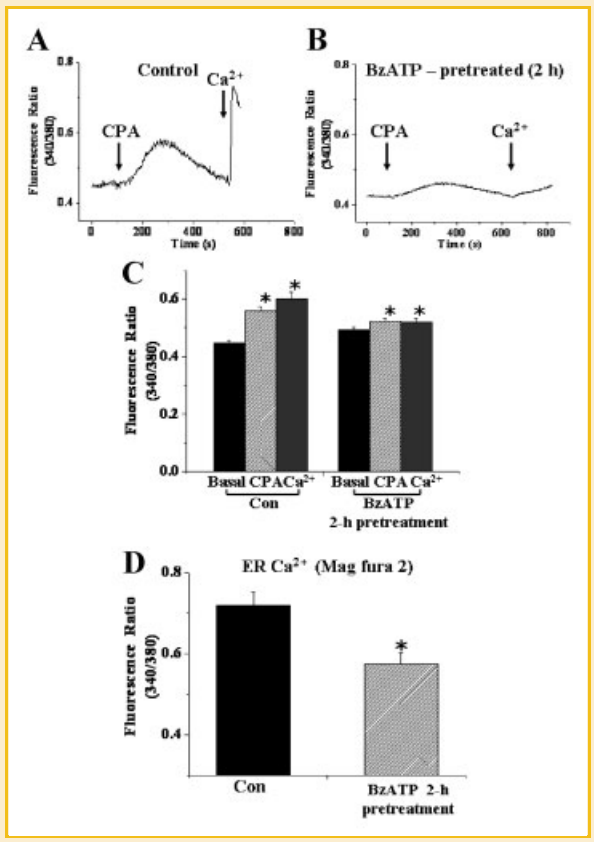

Fig. 4. BzATP pretreatment caused a reduction in CPA-induced Ca^{2+} release and Ca^{2+} influx in differentiated NG108-15 cells. Control cells (A) or cells pretreated with 100 μM BzATP for 2 h and then washed in Ca^{2+}-containing bath solution (B) were assayed for $[Ca^{2+}]_i$ in Ca^{2+}-free bath solution. After CPA (50 μM)-induced Ca^{2+} release, 3 mM Ca^{2+} was added to the bath solution. C: Results from (A) and (B) are quantified. In each group, results are mean ± SEM of 36–54 cells from five separate experiments. Asterisks indicate statistical significance ($P < 0.05$) in comparison to the basal level. D: Cells were treated with or without 100 μM BzATP for 2 h and then assayed for ER Ca^{2+} concentration using Mag fura 2 as dye. Results are mean ± SEM of 23–31 cells from three separate experiments. Asterisks indicate statistical significance ($P < 0.05$) in comparison to the control.

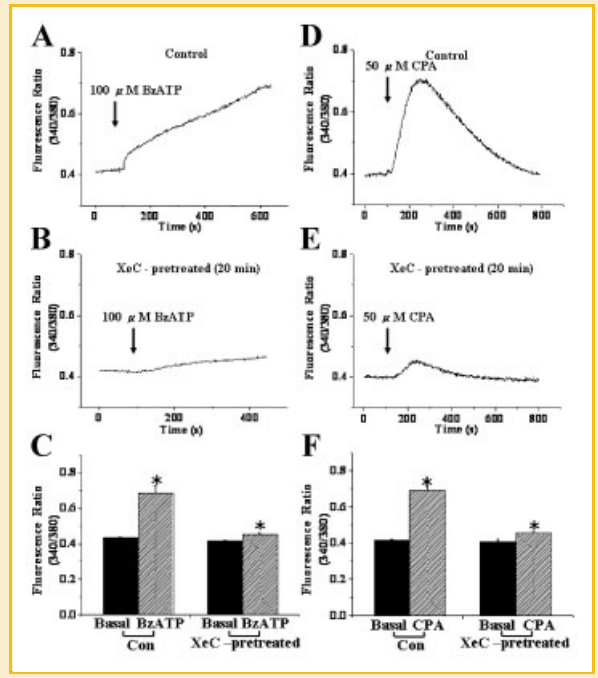

Fig. 5. Effects of XeC on BzATP-triggered Ca^{2+} signal and CPA-induced Ca^{2+} release in differentiated NG108-15 cells. Control cells (A) or cells pretreated with 2 μM XeC for 20 min (B) were assayed for $[Ca^{2+}]_i$ in Ca^{2+}-containing bath solution and challenged with 100 μM BzATP. C: Results from (A) and (B) are quantified. In another set of experiments, control cells (D) or cells pretreated with 2 μM XeC for 20 min (E) were assayed for $[Ca^{2+}]_i$ in Ca^{2+}-free bath solution and treated with 50 μM CPA. F: Results from (D) and (E) are quantified. Results are mean ± SEM of 25–78 cells from four separate experiments. Asterisks indicate statistical significance ($P < 0.05$) in comparison to the basal level.

As the BzATP-triggered Ca^{2+} signal involved Ca^{2+} release via IP3R, could XeC pretreatment (blockade of IP3R) prevent BzATP-induced Ca^{2+} store depletion? We first tested if XeC could be washed away; this was important since if XeC could not be washed away and stayed in the cytosol, it would inhibit CPA-induced Ca^{2+} discharge (see Fig. 5D–F). The cells were pretreated with XeC for 20 min, washed in Ca^{2+}-containing solution and then bathed in Ca^{2+}-free solution; in these cells, CPA-induced Ca^{2+} store discharge was comparable to that observed in control cells (not treated with XeC) (Fig. 6B versus 6A). This indicated that XeC could be effectively washed out. In Figure 6C, after cells were pretreated with 100 μM BzATP for 2 h, CPA-induced Ca^{2+} store discharge was much smaller than that observed in control cells (Fig. 6C versus 6A, $P < 0.05$; also see Fig. 6E and Fig. 4). However, when cells were pretreated with both 100 μM BzATP and 2 μM XeC for 2 h, CPA-induced Ca^{2+} store discharge was largely preserved as compared to the control cells (Fig. 6D,E). These data suggest that blockade of IP3R by XeC pretreatment could prevent Ca^{2+} store depletion induced by BzATP. Consistently, XeC pretreatment could prevent the drop in ER Ca^{2+} level induced by BzATP (Fig. 6F).

The lowered Ca^{2+} concentration in the Ca^{2+} store might induce ER stress. Therefore, an experiment was performed to examine if ER stress markers would appear after BzATP challenge for 2 h and whether XeC could prevent the appearance of these markers. As shown in Figure 7A,B, after BzATP treatment for 2 h cells had high levels of phosphorylated eIF-2α and CHOP, both being ER stress markers [Szegezdi et al., 2006]. XeC pretreatment prevented BzATP-induced appearance of these ER stress markers.

An important question to ask was whether XeC, by preventing Ca^{2+} store depletion and ER stress, could eventually alleviate cell death. The results in Figure 7C revealed that XeC could almost completely reverse the cell death inflicted by 50 μM BzATP (24 h incubation). Evidence also suggested that BzATP-induced cell death was apoptotic, as BzATP insult enhanced the level of cleaved caspase-3 (Fig. 7D,E). XeC co-treatment abrogated such enhancement. Taken together, our data suggested that inhibition of Ca^{2+} release (via IP3R) could protect the Ca^{2+} stores from depletion and prevent BzATP-induced ER stress and apoptotic cell death.

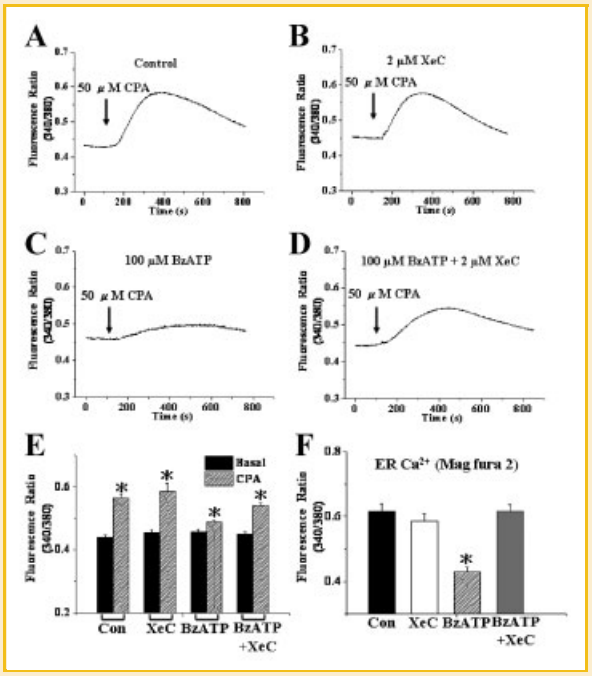

Fig. 6. XeC pretreatment attenuated the reduction in CPA-induced Ca^{2+} release in BzATP-pretreated differentiated NG108-15 cells. A: Control cells in Ca^{2+}-free bath solution were stimulated with 50 μM CPA. B: Cells were pretreated with 2 μM XeC for 20 min. The cells were then washed in Ca^{2+}-containing bath solution, put in Ca^{2+}-free bath solution and subsequently stimulated with 50 μM CPA. C: BzATP (100 μM)-pretreated (2 h) cells were washed in Ca^{2+}-containing bath solution and then bathed in Ca^{2+}-free bath solution and subsequently stimulated with 50 μM CPA. D: Cells were pretreated with 2 μM XeC for 20 min and then with 100 μM BzATP for 2 h. The cells were then washed in Ca^{2+}-containing bath solution, put in Ca^{2+}-free bath solution and subsequently stimulated with 50 μM CPA. E: Results from (A–D) are quantified. Results are mean ± SEM of 19–85 cells from four separate experiments. Asterisks indicate statistical significance ($P < 0.05$) in comparison to the basal level. F: Control cells, cells with 20-min XeC (2 μM) pretreatment, cells with 100 μM BzATP pretreatment (2 h), or cells with 2 μM XeC (20 min) and then with 100 μM BzATP pretreatment (2 h), were assayed for ER Ca^{2+} using Mag fura 2. Results are mean ± SEM of 14–25 cells from three separate experiments. Asterisks indicate statistical significance ($P < 0.05$) in comparison to the control.

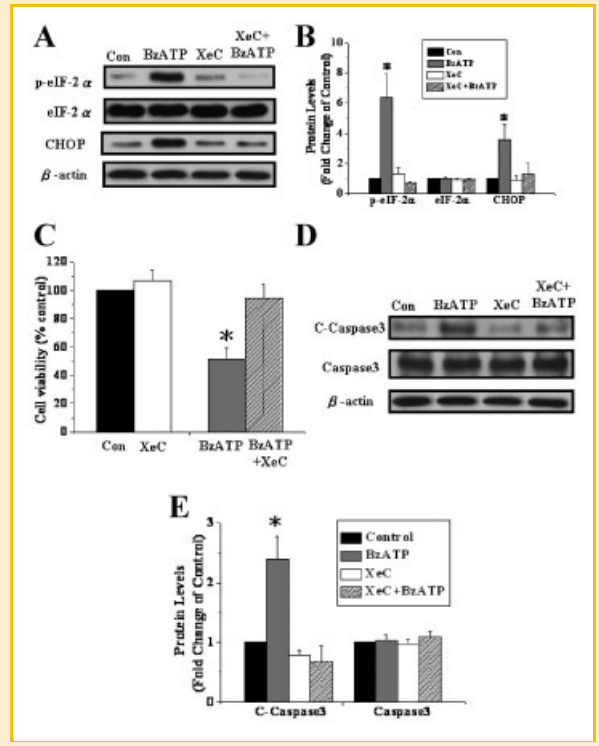

Fig. 7. XeC prevented BzATP-induced lethality and the induction of ER stress and apoptotic markers in BzATP-treated differentiated NG108-15 cells. A: Control cells, cells treated with 100 μM BzATP (2 h), cells treated with 2 μM XeC (2 h), or cells treated with 2 μM XeC and 100 μM BzATP for 2 h, were analyzed for ER stress markers (p-eIF-2α and CHOP) by Western blotting. B: The levels of protein were quantified by densitometry and normalized with β-actin. Results are mean ± SEM from four separate experiments. Asterisks indicate statistical significance ($P < 0.05$) in comparison to the control. C: Control cells, cells treated with 2 μM XeC, cells treated with 50 μM BzATP, or cells treated with 2 μM XeC and 50 μM BzATP (for 24 h) were assayed for cell viability using trypan blue exclusion test. Results are mean ± SEM from four separate experiments. D: Control cells, cells treated with 100 μM BzATP (2 h), cells treated with 2 μM XeC (2 h), or cells treated with 2 μM XeC and 100 μM BzATP for 2 h, were analyzed for cleaved caspase 3 (C-caspase 3, an apoptotic marker) by Western blotting. E: The levels of protein were quantified by densitometry and normalized with β-actin. Results are mean ± SEM from four separate experiments. Asterisks indicate statistical significance ($P < 0.05$) in comparison to the control.

DISCUSSION

Hyperactivation of glutamate receptors, leading to cytosolic Ca^{2+} overload, has been well known to cause neuronal cell death (excitotoxicity) in brain ischemia and in stroke. Whether glutamate-mediated neuroexcitotoxicity involves ER stress, however, still remains controversial and may depend on glutamate receptor subtypes and the types of neurons [Sokka et al., 2007; Concannon et al., 2008; Ruiz et al., 2009]. In recent years, elevated levels of extracellular ATP, acting via P2X7R, have been increasingly recognized as a neurotoxic signal in brain ischemia and spinal cord injury [Wang et al., 2004; Matute et al., 2007; Peng et al., 2009; Skaper et al., 2010]. P2X7R channel opening allows sustained Na^{+} and Ca^{2+} influx and consequently Ca^{2+} overload [Browne et al., 2010]. Hitherto no information is available on whether P2X7R-mediated neurotoxicity involves perturbation of organelle Ca^{2+} and ER stress. Here we provide the first report to show that P2X7R stimulation could lead to sustained Ca^{2+} store depletion, ER stress and apoptotic cell death. Suppression of Ca^{2+} release by IP3R blockade prevented P2X7R-induced Ca^{2+} store depletion, ER stress, and apoptotic cell death.

Treatment of cells with BzATP for only 2 h did not result in cell death (Fig. 1B) but had already allowed cytotoxic signals to be inflicted onto the cells (Fig. 1C). Ca^{2+} signals triggered by BzATP were slow (Fig. 2A–D) and may reflect the gradual dilation of the P2X7R pore [Browne et al., 2010]. After 2 h of BzATP treatment, $[Ca^{2+}]_i$ still remained high in the presence of BzATP (Fig. 2E). BzATP-induced damage did not appear to occur at the plasmalemma: Washing out BzATP led to a recovery of $[Ca^{2+}]_i$ back to a resting level comparable to that of the control (Fig. 3), suggesting Ca^{2+}

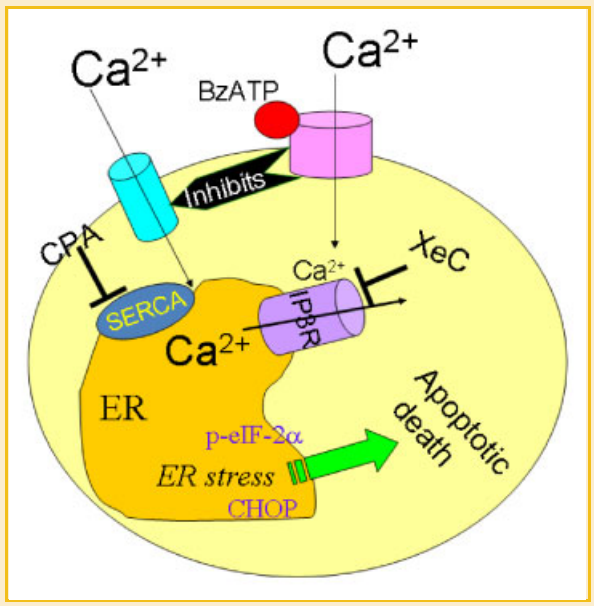

Fig. 8. A schematic illustration of the cellular components involved in P2X7R-mediated neurotoxicity. Binding of BzATP to P2X7R causes Ca^{2+} influx, which sensitizes IP3R and triggers more release of Ca^{2+} from the ER. The reduced Ca^{2+} content in the ER causes ER stress with the induction of ER stress markers (phosphorylated eIF-2α and CHOP) and eventually apoptotic cell death. Activation of P2X7R by BzATP, via undefined signaling pathways, also causes inhibition of store-operated Ca^{2+} entry; such inhibition may account for the failure of the ER to be refilled with Ca^{2+} after depletion. Two drug tools, namely, CPA and XeC, were used in this study. CPA inhibits SERCA and thus could release Ca^{2+} from the ER. XeC is an antagonist of IP3R; in this work XeC has been shown to prevent Ca^{2+} store depletion, ER stress, and apoptotic death after BzATP challenge. [Color figure can be seen in the online version of this article, available at http://wileyonlinelibrary.com/journal/jcb]

clearance mechanisms still remained vigorous. Together with the comparable Ca^{2+} responses to high KCl (which opened plasmalemmal voltage-gated Ca^{2+} channels) (Fig. 3), the data suggest that the plasma membrane still maintained functional integrity after 2 h of BzATP challenge.

What could be the damage after a 2-h BzATP treatment? Results in Figure 4A–C suggest that such treatment resulted in Ca^{2+} store depletion, consistent with the reduced ER Ca^{2+} concentration (Fig. 4D). The observation that XeC substantially inhibited BzATP-triggered $[Ca^{2+}]_i$ elevation (Fig. 5) suggests that P2X7R activation also led to intracellular Ca^{2+} release via IP3R. Since BzATP did not induce Ca^{2+} signal in Ca^{2+}-free bath solution, the data suggest that BzATP initially triggered Ca^{2+} influx, which then induced Ca^{2+} release from the internal stores via sensitizing IP3R. This is similar to the Ca^{2+}-induced Ca^{2+} release mechanism in the case of ryanodine-receptor channel as cytosolic Ca^{2+} acts as a co-agonist at both the IP3R and RYR [Lee, 2004; Berridge, 2009]. Since caffeine (20 mM) did not trigger any Ca^{2+} release (not shown), differentiated NG108-15 cells seemed to be devoid of functional ryanodine receptor channels. Thus, although differentiated NG108-15 cells have developed extensive neurites typical of neuronal morphology, the absence of functional RYR suggests that these cells may not have developed the full repertoire of Ca^{2+} signaling mechanisms expected of mature primary neurons.

By suppressing BzATP-triggered Ca^{2+} release, XeC co-treatment largely preserved the functional size of the CPA-dischargeable pool (Fig. 6A–E). This is supported by the finding that XeC co-treatment also abrogated the effect of BzATP in lowering ER Ca^{2+} concentration (Fig. 6F). Consistently, XeC co-treatment prevented the appearance of ER stress markers (phosphorylated eIF-2α and CHOP) upon BzATP challenge (Fig. 7A,B). Most significantly, XeC could reverse the cytotoxic effect and suppress the appearance of apoptotic marker (cleaved caspase-3) after BzATP insult (Fig. 7C–E). Taken together, the data suggest that P2X7R stimulation led to IP3R-mediated Ca^{2+} release, Ca^{2+} store depletion, ER stress and eventually apoptotic cell death (see schematic diagram in Fig. 8).

It still remains unclear how IP3R-mediated Ca^{2+} release led to sustained Ca^{2+} store depletion. The empty state of the Ca^{2+} store presumably could activate store-operated Ca^{2+} entry, which would refill the Ca^{2+} store. Results in Figure 4 reveal that SOC was in fact inhibited in BzATP-treated cells. The cause for this inhibition is unknown. The SOC is now believed to be composed of the proteins STIM (as a sensor of the Ca^{2+} content in the store) and Orai (the channel protein at the plasma membrane tethered to and activated by STIM) [Varnai et al., 2009]. Further work is warranted to examine if there is an uncoupling of the store status to the plasmalemma.

IP3R-mediated intracellualar Ca^{2+} release triggered by Ca^{2+} influx appears in several receptors and cell types. For instance, in renal vascular smooth muscle cells, activation of P2X receptors by the selective agonist αβ-methylene ATP depolarizes the membrane, triggers the opening of voltage-gated Ca^{2+} channels, the Ca^{2+} influx subsequently activates IP3R-mediated Ca^{2+} release in sub-plasmalemmal sarcoplasmic reticulum [Povstyan et al., 2011]. In human fetal astrocytes, influx of Ca^{2+} via P2 purinoceptors activated by di(adenosine-5′) pentaphosphate causes Ca^{2+} release through both IP3R and RYR [Holden et al., 2000]. In human SH-SY5Y neuroblastoma cells, nicotinic cholinoceptor-triggered depolarization was followed by opening of voltage-gated Ca^{2+} channels, subsequent Ca^{2+} influx also activates IP3R and RYR [Dajas-Bailador et al., 2002]. However, it is unknown in the above cases whether Ca^{2+} store depletion, ER stress, or cytotoxicity took place.

It has been reported that stimulation of the receptors for α-amino- 3-hydroxy-5-methyl-4-isoxazolepropionic acid (AMPA receptor, an ionotropic glutamate receptor subtype) causes ER stress, Ca^{2+} overload, and cytotoxicity in oligodendrocytes [Ruiz et al., 2010]. In this work, pharmacological inhibition of RYR, but not of IP3R, could reduce Ca^{2+} overload and cell death, suggesting the involvement of RYR-mediated Ca^{2+} release in AMPA receptor-triggered excitotoxicity. In cortical neurons, Ca^{2+} release via both RYR and IP3R is involved in NMDA-induced Ca^{2+} overload, ER stress, and cell death [Ruiz et al., 2009]. Our work shows that P2X7R-mediated ER stress and cell death in differentiated neuronal NG108-15 cells involved Ca^{2+} release through IP3R but not RYR. Hence, the accumulating evidence suggests that Ca^{2+} flux via intracellular Ca^{2+} release channels is involved in cytosolic Ca^{2+} overload and ER stress in excitotoxicity.

It is of importance to note that stimulation of P2X7R not only triggers Ca^{2+} entry, but also leads to activation of extracellular signal-regulated kinases (ERK1/2), c-Jun N-terminal kinases (JNK), and p38 mitogen-activated protein kinases (MAPK) in various cell

types [Amstrup and Novak, 2003; Pfeiffer et al., 2004; Stefano et al., 2007; Shiratori et al., 2010]. When WT and mutant P2X7R are heterologously expressed in HEK-293 cells, it has been shown that the N-terminus, but not the C-terminus, is important in ERK activation [Amstrup and Novak, 2003]. Whether P2X7R also stimulates ERK, JNK, and p38 MAPK in differentiated NG108-15 cells, and whether there is a link between these signaling pathway(s) and sustained Ca^{2+} store depletion after BzATP challenge, will await further investigation.

In conclusion, our work presents novel data showing that Ca^{2+} release via IP3R, sustained Ca^{2+} store depletion and ER stress were involved in P2X7R-mediated neurotoxicity.

ACKNOWLEDGMENTS

YML thanks the National Science Council of Taiwan for research support (NSC 100-2320-B-039-006-). CCC is a recipient of a Hsing Tian Kong Scholarship. KLW would like to thank China Medical University Hospital for support (DMR-97-101).

REFERENCES

Amstrup J, Novak I. 2003. P2X7 receptor activates extracellular signal-regulated kinases ERK1 and ERK2 independently of Ca^{2+} influx. Biochem J 374:51–61.

Berridge MJ. 2009. Inositol trisphosphate and calcium signalling mechanisms. Biochim Biophys Acta 1793:933–940.

Browne LE, Jiang LH, North RA. 2010. New structure enlivens interest in P2X receptors. Trends Pharmacol Sci 31:229–237.

Cavaliere F, Sancesario G, Bernardi G, Volonte C. 2002. xtracellular ATP and nerve growth factor intensify hypoglycemia-induced cell death in primary neurons: Role of P2 and NGFRp75 receptors. J Neurochem 83:1129–1138.

Concannon CG, Ward MW, Bonner HP, Kuroki K, Tuffy LP, Bonner CT, Woods I, Engel T, Henshall DC, Prehn JH. 2008. NMDA receptor-mediated excitotoxic neuronal apoptosis in vitro and in vivo occurs in an ER stress and PUMA independent manner. J Neurochem 105:891–903.

Dajas-Bailador FA, Mogg AJ, Wonnacott S. 2002. Intracellular Ca^{2+} signals evoked by stimulation of nicotinic acetylcholine receptors in SH-SY5Y cells: Contribution of voltage-operated Ca^{2+} channels and Ca^{2+} stores. J Neurochem 81:606–614.

Franke H, Gunther A, Grosche J, Schmidt R, Rossner S, Reinhardt R, Faber-Zuschratter H, Schneider D, Illes P. 2004. P2X7 receptor expression after ischemia in the cerebral cortex of rats. J Neuropathol Exp Neurol 63: 686–699.

Gerasimenko O, Tepikin A. 2005. How to measure Ca^{2+} in cellular organelles? Cell Calcium 38:201–211.

Harding HP, Ron D. 2002. Endoplasmic reticulum stress and the development of diabetes: A review. Diabetes 51 (Suppl 3): S455–S461.

Holden CP, Haughey NJ, Dolhun B, Shepel PN, Nath A, Geiger JD. 2000. Diadenosine pentaphosphate increases levels of intracellular calcium in astrocytes by a mechanism involving release from caffeine/ryanodine- and IP_3-sensitive stores. J Neurosci Res 59:276–282.

Hu H, Lu W, Zhang M, Zhang X, Argall AJ, Patel S, Lee GE, Kim YC, Jacobson KA, Laties AM, Mitchell CH. 2010. Stimulation of the P2X7 receptor kills rat retinal ganglion cells in vivo. Exp Eye Res 91:425–432.

Jarvis MF, Khakh BS. 2009. ATP-gated P2X cation-channels. Neuropharmacology 56:208–215.

Lee HC. 2004. Multiplicity of Ca^{2+} messengers and Ca^{2+} stores: A perspective from cyclic ADP-ribose and NAADP. Curr Mol Med 4:227–237.

Leung YM, Huang CF, Chao CC, Lu DY, Kuo CS, Cheng TH, Chang LY, Chou CH. 2011. Voltage-gated K^+ channels play a role in cAMP-stimulated neuritogenesis in mouse neuroblastoma N2A cells. J Cell Physiol 226: 1090–1098.

Leung YM, Kwan TK, Kwan CY, Daniel EE. 2002. Calyculin A-induced endothelial cell shape changes are independent of [Ca(2+)](i) elevation and may involve actin polymerization. Biochim Biophys Acta 1589:93–103.

Lu DY, Yu WH, Yeh WL, Tang CH, Leung YM, Wong KL, Chen YF, Lai CH, Fu WM. 2009. Hypoxia-induced matrix metalloproteinase-13 expression in astrocytes enhances permeability of brain endothelial cells. J Cell Physiol 220:163–173.

Matute C, Alberdi E, Domercq M, Sanchez-Gomez MV, Perez-Samartin A, Rodriguez-Antiguedad A, Perez-Cerda F. 2007. Excitotoxic damage to white matter. J Anat 210:693–702.

Peng W, Cotrina ML, Han X, Yu H, Bekar L, Blum L, Takano T, Tian GF, Goldman SA, Nedergaard M. 2009. Systemic administration of an antagonist of the ATP-sensitive receptor P2X7 improves recovery after spinal cord injury. Proc Natl Acad Sci USA 106:12489–12493.

Pfeiffer ZA, Aga M, Prabhu U, Watters JJ, Hall DJ, Bertics PJ. 2004. The nucleotide receptor P2X7 mediates actin reorganization and membrane blebbing in RAW 264.7 macrophages via p38 MAP kinase and Rho. J Leukoc Biol 75:1173–1182.

Povstyan OV, Harhun MI, Gordienko DV. 2011. Ca^{2+} entry following P2X receptor activation induces IP_3 receptor-mediated Ca^{2+} release in myocytes from small renal arteries. Br J Pharmacol 162:1618–1638.

Ruiz A, Matute C, Alberdi E. 2009. Endoplasmic reticulum Ca(2+) release through ryanodine and IP(3) receptors contributes to neuronal excitotoxicity. Cell Calcium 46:273–281.

Ruiz A, Matute C, Alberdi E. 2010. Intracellular Ca^{2+} release through ryanodine receptors contributes to AMPA receptor-mediated mitochondrial dysfunction and ER stress in oligodendrocytes. Cell Death Dis 1:e54.

Shiratori M, Tozaki-Saitoh H, Yoshitake M, Tsuda M, Inoue K. 2010. P2X7 receptor activation induces CXCL2 production in microglia through NFAT and PKC/MAPK pathways. J Neurochem 114:810–819.

Skaper SD, Debetto P, Giusti P. 2010. The P2X7 purinergic receptor: From physiology to neurological disorders. FASEB J 24:337–345.

Sokka AL, Putkonen N, Mudo G, Pryazhnikov E, Reijonen S, Khiroug L, Belluardo N, Lindholm D, Korhonen L. 2007. Endoplasmic reticulum stress inhibition protects against excitotoxic neuronal injury in the rat brain. J Neurosci 27:901–908.

Stefano L, Rossler OG, Griesemer D, Hoth M, Thiel G. 2007. P2X(7) receptor stimulation upregulates Egr-1 biosynthesis involving a cytosolic Ca(2+) rise, transactivation of the EGF receptor and phosphorylation of ERK and Elk-1. J Cell Physiol 213:36–44.

Sugiyama T, Oku H, Shibata M, Fukuhara M, Yoshida H, Ikeda T. 2010. Involvement of P2X7 receptors in the hypoxia-induced death of rat retinal neurons. Invest Ophthalmol Vis Sci 51:3236–3243.

Szegezdi E, Logue SE, Gorman AM, Samali A. 2006. Mediators of endoplasmic reticulum stress-induced apoptosis. EMBO Rep 7:880–885.

Varnai P, Hunyady L, Balla T. 2009. STIM and Orai: The long-awaited constituents of store-operated calcium entry. Trends Pharmacol Sci 30: 118–128.

Wang X, Arcuino G, Takano T, Lin J, Peng WG, Wan P, Li P, Xu Q, Liu QS, Goldman SA, Nedergaard M. 2004. P2X7 receptor inhibition improves recovery after spinal cord injury. Nat Med 10:821–827.

Watano T, Matsuoka I, Ogawa K, Kimura J. 2002. Effects of anions on ATP-induced [Ca2+], increase in NG108-15 cells. Jpn J Pharmacol 89:302–308.

Wirkner K, Kofalvi A, Fischer W, Gunther A, Franke H, Groger-Arndt H, Norenberg W, Madarasz E, Vizi ES, Schneider D, Sperlagh B, Illes P. 2005. Supersensitivity of P2X receptors in cerebrocortical cell cultures after in vitro ischemia. J Neurochem 95:1421–1437.